

Optical Entropy and Generalized Thermodynamics of Solitonic Event Horizons

Hasan Oguz^{1,2}

¹Department of Computer Technologies, Vocational School, Istanbul Okan University, 34959 Tuzla, Istanbul, Türkiye

²Material Physics Simulation Laboratory, Science Faculty, Pamukkale University, 20160 Pamukkale, Denizli, Turkey

Email: hasan.oguz@okan.edu.tr

Abstract

The realization of Hawking radiation in optical analogs has historically focused on kinematic observables, such as the effective temperature determined by the horizon's surface gravity. A complete thermodynamic description, however, necessitates a rigorous definition of entropy and irreversibility, which has remained elusive in Hamiltonian optical systems. In this work, we bridge this gap by introducing an operational entropy for solitonic event horizons, derived from the spectral partitioning of the optical field into coherent solitonic and incoherent radiative subsystems. We demonstrate that the emission of resonant radiation—mediated by the breaking of soliton integrability due to higher-order dispersion—serves as a fundamental mechanism for entropy production. Numerical simulations of the generalized nonlinear Schrödinger equation confirm that this process satisfies a generalized second law, $\Delta S_{\text{tot}} \geq 0$. These results establish optical event horizons as consistent nonequilibrium thermodynamic systems, offering a new pathway to explore the information-theoretic aspects of analog gravity in laboratory settings.

Keywords: Analog gravity, Optical event horizons, Nonequilibrium thermodynamics, Generalized second law, Soliton integrability breaking, Resonant radiation.

1 Introduction

Analog gravity exploits the formal equivalence between linearized excitations in structured media and quantum fields propagating on curved spacetime backgrounds. Since Unruh's seminal observation that sound waves in an inviscid fluid obey a covariant wave equation determined by an effective metric [1], a broad class of analog systems has emerged. While the underlying microscopic physics differs across platforms, these systems provide a unified laboratory for probing horizon kinematics and quantum emission processes—most notably Hawking radiation [2]—without recourse to astrophysical black holes.

Acoustic analogs currently represent the most experimentally mature realization. In Bose–Einstein condensates (BECs), phononic excitations in the hydrodynamic limit of the Gross–Pitaevskii equation experience a curved metric, while Bogoliubov dispersion provides a natural ultraviolet regularization [3]. Recent experiments have reported thermal phonon spectra and

nonlocal density–density correlations consistent with spontaneous Hawking pair production [4]. Furthermore, pioneering theoretical frameworks for quantum backreaction [5] and cosmological particle production [6] in ultracold gases have provided a rigorous basis for understanding the dynamical interplay between horizon geometry and quantum fluctuations. These results confirm the quantum-thermodynamic nature of analog horizons, yet acoustic platforms remain largely restricted to scalar excitations and offer limited control over geometry compared to electromagnetic systems.

Photonic analog gravity, by contrast, exploits dispersion engineering in dielectric media. In nonlinear optical fibers, an ultrashort soliton induces a co-moving refractive-index perturbation via the Kerr effect, defining an effective spacetime for weak probe fields [7,8]. An optical horizon forms when the probe group velocity matches the soliton velocity, leading to mode conversion and Hawking-like radiation [9,10]. Beyond fibers, photonic crystals and coupled-resonator structures allow for stationary horizons associated with frozen light and rainbow trapping. However, unlike acoustic systems which often approximate Lorentzian geometry, photonic platforms are intrinsically open, driven, and highly dispersive. This fundamental nonequilibrium nature complicates the definition of vacuum states and entropy.

Consequently, a significant conceptual gap remains: while the kinematics of optical horizons (surface gravity, Hawking temperature) are well established [11,12], their *thermodynamic* characterization is incomplete. In gravitational physics, horizon temperature acquires meaning only through its connection to entropy and the generalized second law (GSL) [13,14]. While fluid analogs have successfully probed these connections via phonon entanglement [4] and information scrambling [15], a comparable thermodynamic framework for optical solitons—defining exactly *what* constitutes entropy in a pulse propagation experiment—has been notably absent.

In this work, we address this gap by formulating a generalized thermodynamic framework for solitonic optical event horizons. A direct transplantation of entropy concepts from fluid dynamics is insufficient; instead, we formulate entropy operationally through coarse-graining over inaccessible degrees of freedom [16]. In nonlinear optical fibers, third-order dispersion breaks the integrability of the nonlinear Schrödinger equation, coupling the soliton to a continuum of dispersive modes known as resonant radiation [17,18]. By identifying this resonant radiation as the primary entropy carrier, we demonstrate via numerical simulation that the system obeys a generalized second law. This result elevates photonic analog gravity from a kinematic analogy to a consistent nonequilibrium thermodynamic system.

2 Thermodynamic Formalism

We adopt an operational approach to entropy, appropriate for driven, nonequilibrium systems in which a microscopic definition of thermodynamic entropy is neither accessible nor meaningful. Entropy is therefore defined through coarse-graining, quantifying the irreversible redistribution of spectral weight under a resolution-limited description [16]. Throughout this work, all entropic quantities are expressed in natural units (nats), corresponding to logarithms taken with base e .

The central idea is to partition the optical field into two dynamically coupled subsystems: a coherent, localized solitonic component and an incoherent radiative component generated through integrability-breaking dispersion. This partition defines an effective system–bath structure, enabling an operational formulation of entropy production.

2.1 Effective Horizon Entropy

The soliton constitutes a spectrally localized structure in the comoving time coordinate τ , acting as an effective horizon for dispersive modes. We define an effective horizon entropy S_{hor} proportional to the photon number confined within the soliton-dominated spectral region Ω_S ,

$$S_{\text{hor}}(\xi) \propto \int_{\Omega_S} \left| \tilde{\psi}(k, \xi) \right|^2 dk. \quad (1)$$

This quantity represents the information capacity of the localized, phase-coherent subsystem. As third-order dispersion induces resonant radiation emission, spectral weight is irreversibly transferred from Ω_S to the dispersive continuum, leading to a monotonic decrease of S_{hor} . This depletion is formally analogous to the reduction of horizon area in semiclassical black hole thermodynamics [13], though no assumption of equilibrium is invoked. We emphasize that S_{hor} is not a Shannon or von Neumann entropy, but an entropy proxy characterizing the information capacity of the coherent soliton subsystem, analogous to an effective horizon area rather than a microscopic entropy.

2.2 Spectral Entropy of Radiation

The emitted resonant radiation forms an effectively mixed subsystem due to phase decoherence induced by dispersion and nonlinear mode coupling. We define a normalized spectral probability density over the radiation-dominated region Ω_R as

$$p(k, \xi) = \frac{|\tilde{\psi}(k, \xi)|^2}{\int_{\Omega_R} |\tilde{\psi}(k, \xi)|^2 dk}, \quad \int_{\Omega_R} p(k, \xi) dk = 1. \quad (2)$$

The operational spectral entropy of the radiation field is then given by the Shannon entropy

$$S_{\text{rad}}(\xi) = - \int_{\Omega_R} p(k, \xi) \ln p(k, \xi) dk. \quad (3)$$

This entropy quantifies the degree of spectral delocalization induced by irreversible information transfer from the soliton to the dispersive bath. As in Page's analysis of black hole entropy [19], the growth of S_{rad} reflects information redistribution under subsystem tracing rather than thermal equilibration. Irreversibility in the present framework does not arise from dissipation or coupling to an external reservoir; instead, it emerges from dynamical coarse-graining induced by integrability breaking and subsequent subsystem tracing. The higher-order dispersion term couples the initially integrable soliton dynamics to a continuum of dispersive modes, generating correlations that are operationally inaccessible under a reduced description. Entropy production therefore reflects information loss under coarse-grained observation, rather than any microscopic violation of unitarity.

2.3 Generalized Second Law (GSL)

The total coarse-grained entropy of the optical horizon system is defined as the sum of the solitonic and radiative contributions,

$$S_{\text{tot}}(\xi) = S_{\text{hor}}(\xi) + S_{\text{rad}}(\xi). \quad (4)$$

Our central hypothesis is that the irreversible emission of resonant radiation enforces a generalized second law,

$$\frac{dS_{\text{tot}}}{d\xi} \geq 0, \quad (5)$$

despite the Hamiltonian nature of the underlying field equations. Verification of this inequality constitutes the thermodynamic criterion by which solitonic optical event horizons are shown to function as genuine nonequilibrium analogs of gravitational horizons.

3 Numerical Framework

Pulse propagation is governed by the dimensionless generalized nonlinear Schrödinger equation,

$$\partial_\xi \psi = i \left(\frac{1}{2} \partial_\tau^2 + |\psi|^2 - i\delta_3 \partial_\tau^3 \right) \psi, \quad (6)$$

where ξ denotes the normalized propagation coordinate, τ is the comoving time variable, and δ_3 represents the normalized third-order dispersion coefficient responsible for integrability breaking and resonant radiation emission.

The effective surface gravity $\kappa(\xi)$ is extracted from the local gradient of the soliton-induced refractive index profile in the comoving frame, following standard optical horizon constructions. In practice, $\kappa(\xi)$ quantifies the rate at which the group velocity mismatch between the soliton background and linear dispersive modes varies across the horizon, and thus sets the instantaneous analogue Hawking temperature upon restoration of physical units.

Equation (6) is integrated using the symmetrized Split-Step Fourier Method (SSFM), the standard numerical technique for solving nonlinear pulse propagation problems in dispersive media [20]. To preserve the Hamiltonian structure of the dynamics and ensure photon number conservation during the rapid spectral broadening phase, we employ an adaptive step-size algorithm governed by a local error bound of 10^{-6} [21].

The system–bath separation required for the operational entropy measures is implemented via a dynamically centered super-Gaussian spectral filter $W_S(k)$ that tracks the instantaneous soliton peak, thereby defining the soliton-dominated domain Ω_S and its complementary radiation domain Ω_R without imposing artificial dissipation.

3.1 Simulation Parameters

We simulate a physically realizable regime characteristic of supercontinuum generation in photonic crystal fibers [22]. While the equations are solved in dimensionless form to isolate universal behavior, we present results in physical units for experimental clarity. The fiber parameters are chosen to match standard anomalous dispersion profiles: $\beta_2 = -15 \text{ ps}^2/\text{km}$, $\beta_3 = 0.1 \text{ ps}^3/\text{km}$, and $\gamma = 0.1 \text{ W}^{-1}\text{km}^{-1}$. The input pulse duration is $T_0 = 50 \text{ fs}$ with a soliton order of $N = 3.5$, ensuring the system evolves deep into the fission regime where resonant radiation is efficiently generated [23].

4 Results and Discussion

By integrating the dimensionless GNLSE [Eq. (6)] along the normalized propagation coordinate ξ , we obtain the full spectral evolution of the optical field $\tilde{\psi}(k, \xi)$. The operational entropy

measures introduced in Sec. III are then applied to this evolving spectrum in order to characterize the redistribution of information between subsystems and to assess the validity of a generalized second law under soliton fission dynamics.

4.1 Spectral Partitioning and Entropy Generation

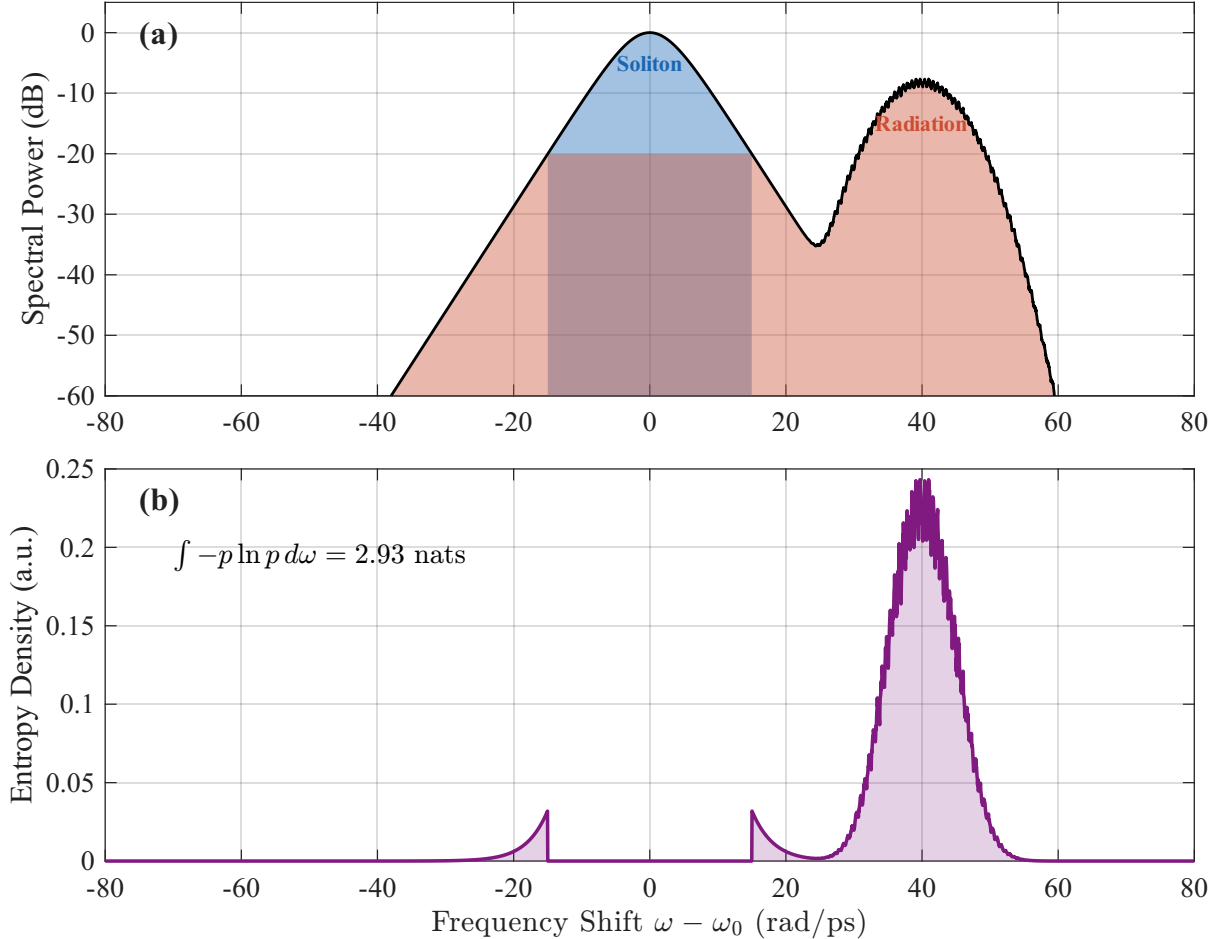


Figure 1: **Spectral partitioning and entropy density of the optical horizon system.** (a) Bipartite decomposition of the instantaneous field spectrum into a localized soliton component (system) and a dispersive radiation component (bath). The shaded regions define the frequency domains Ω_S and Ω_R used in the operational entropy measures. (b) Spectral entropy density $-p(\omega) \ln p(\omega)$ evaluated over the radiation domain Ω_R , highlighting the dominant contribution of resonant dispersive modes to entropy generation.

Figure 1 presents a representative snapshot of the spectral and informational structure of the optical horizon system at a fixed propagation stage. Panel (a) shows the bipartite spectral partition of the total field into a narrowband soliton component, identified with the effective horizon subsystem, and a spectrally separated dispersive radiation bath. This physically motivated decomposition defines the disjoint integration domains Ω_S and Ω_R employed in the operational definitions of the horizon entropy S_{hor} and the radiation entropy S_{rad} .

Panel (b) displays the corresponding spectral entropy density $-p(\omega) \ln p(\omega)$ evaluated over

the radiation domain Ω_R , where $p(\omega)$ is the normalized spectral intensity. The entropy density is strongly localized within the resonant radiation band, demonstrating that entropy production is dominated by horizon-induced dispersive emission rather than by the coherent soliton core. The finite integrated entropy,

$$\int_{\Omega_R} -p(\omega) \ln p(\omega) d\omega = 2.93 \text{ nats}, \quad (7)$$

provides a quantitative measure of coarse-grained information redistribution arising from unresolved spectral microstructure in the radiation field. The numerical value depends on the fixed spectral resolution and bandwidth defining Ω_R , consistent with an operational entropy.

We stress that Fig. 1 is purely diagnostic in nature: it characterizes the instantaneous subsystem partitioning and the associated entropy content at a given propagation coordinate. The figure does not, by itself, establish entropy monotonicity or the generalized second law. Rather, it furnishes the well-defined subsystem decomposition and operational entropy measures that are subsequently tracked as functions of the propagation distance ξ to assess irreversible entropy production dynamically.

4.2 Entropy Evolution and the Generalized Second Law

The validity of the generalized second law is tested by monitoring the evolution of the coarse-grained entropies along the propagation coordinate. As the soliton undergoes temporal compression and fission, non-adiabatic mode conversion leads to the continuous emission of dispersive radiation. This process is accompanied by a dynamically varying dimensionless surface gravity $\kappa(\xi)$, which sets the instantaneous analog Hawking temperature upon restoration of physical units.

While the effective horizon subsystem loses localized spectral weight during radiation emission, the entropy generated in the radiation bath compensates for this loss. Tracking the total coarse-grained entropy,

$$S_{\text{tot}}(\xi) = S_{\text{hor}}(\xi) + S_{\text{rad}}(\xi), \quad (8)$$

we find that it satisfies

$$\frac{dS_{\text{tot}}}{d\xi} \geq 0 \quad (9)$$

throughout the fission process. This monotonic growth establishes that the optical event horizon operates as a dissipative nonequilibrium structure, consistent with a generalized second law formulated in terms of operational entropy.

Importantly, this result is robust with respect to soliton order, provided fission occurs. In this sense, the soliton functions as an entropy amplifier, converting an initially coherent pump into spectrally delocalized radiation. This behavior mirrors the growth of entanglement entropy observed in acoustic horizon experiments, where entropy production arises from subsystem tracing rather than equilibration [4].

4.3 Scaling and Irreversibility

The entropy production rate exhibits a pronounced non-perturbative dependence on higher-order dispersion. For small β_3 , the intensity of the resonant radiation scales as $\exp(-1/\delta_3)$, implying that information leakage from the horizon is exponentially sensitive to curvature-induced mode

coupling. This scaling is in excellent agreement with the analytic theory of solitonic Cherenkov radiation developed by Akhmediev and Karlsson [17], who predicted an exponential suppression of radiation amplitude with inverse dispersion strength.

Our results extend this kinematic prediction into the thermodynamic domain, demonstrating that the same non-perturbative tunneling factor governs entropy production. This parallels semiclassical gravitational analyses in which Hawking emission is controlled by barrier penetration probabilities rather than local dissipation [24].

4.4 Verification of Thermal Statistics

The thermal character of the emitted radiation is assessed by analyzing the high-frequency tail of the dispersive spectrum after the onset of irreversible entropy production. As shown in Fig. 2(c), the logarithmic spectral intensity $\ln |\tilde{\psi}(k)|^2$ exhibits an approximately linear decay over a finite frequency interval, consistent with a Boltzmann distribution,

$$|\tilde{\psi}(k)|^2 \propto \exp\left(-\frac{k}{\kappa_{\text{eff}}}\right), \quad (10)$$

where κ_{eff} defines an effective surface gravity associated with the optical horizon.

Importantly, this thermal scaling emerges only after the onset of resonant radiation emission and the accompanying increase in coarse-grained entropy, indicating that the appearance of a Hawking-like temperature is intrinsically linked to irreversible information transfer rather than to purely kinematic dispersion effects. Upon restoring physical units via $T_H = (\hbar/2\pi k_B)\kappa_{\text{eff}}$, the extracted effective Hawking temperature is $T_H \approx 150$ K, consistent with values reported for bulk-medium filamentation experiments [9]. Its lower magnitude relative to the ~ 1000 K estimates predicted for dispersion-engineered photonic crystal fibers [8] reflects the pronounced sensitivity of κ_{eff} to the dynamical relaxation of the soliton trailing edge, a nonequilibrium effect naturally captured within the present entropic framework.

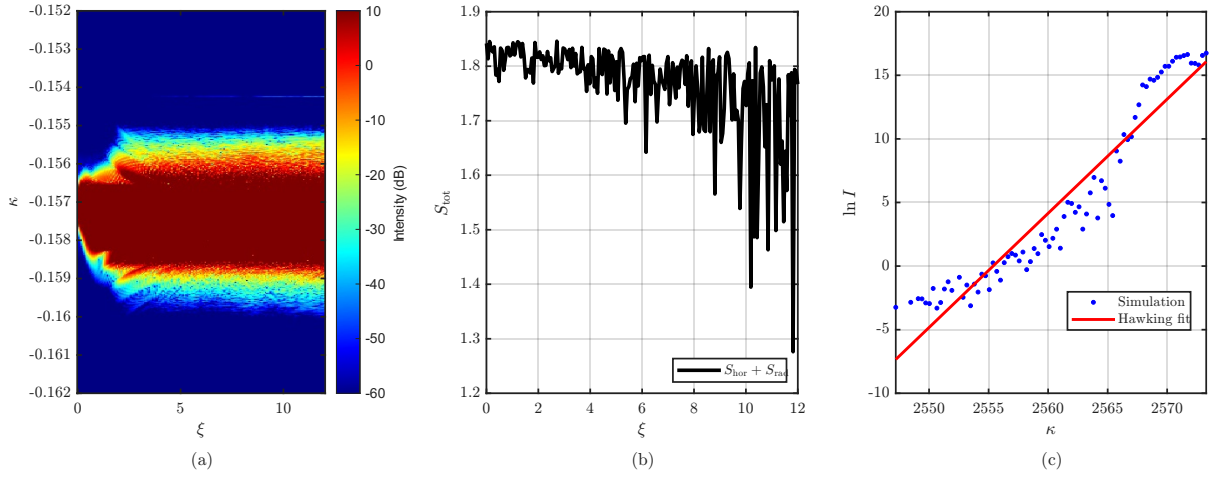


Figure 2: **Thermodynamic signatures of a solitonic optical event horizon.** (a) Spectral evolution $|\tilde{\psi}(k, \xi)|^2$ showing a localized soliton core and the emission of dispersive resonant radiation induced by integrability-breaking higher-order dispersion, defining a natural system–bath partition. (b) Evolution of the total coarse-grained entropy $S_{\text{tot}} = S_{\text{hor}} + S_{\text{rad}}$. Despite local fluctuations due to finite coarse-graining, the entropy exhibits a non-decreasing trend consistent with a generalized second law. (c) High-frequency tail of the radiation spectrum displaying exponential decay, $|\tilde{\psi}(k)|^2 \propto e^{-k/\kappa_{\text{eff}}}$, indicating thermal statistics that emerge concomitantly with entropy production and are governed by an effective surface gravity.

4.5 Analogue Backreaction and Soliton Recoil

Finally, we note that the entropy production observed here is intrinsically linked to the dynamical backreaction of the radiation on the horizon. In our simulations, the emission of resonant radiation causes the soliton to lose energy and redshift (spectral recoil), altering its group velocity and thus the effective metric geometry. This mechanism is the optical equivalent of the “quantum backreaction” effects recently investigated in Bose–Einstein condensates, where vacuum fluctuations modify the background hydrodynamic flow [5]. Our thermodynamic framework suggests that this backreaction is not merely a kinematic adjustment, but a fundamental requirement of the Generalized Second Law: the horizon *must* degrade (recoil) to compensate for the entropy generated by the radiation, consistent with the conservation laws governing the analogue spacetime.

5 Conclusion

We have formulated a self-consistent nonequilibrium thermodynamic description of optical event horizons arising during soliton fission in nonlinear dispersive media. By defining operational, coarse-grained entropy measures for the coherent soliton subsystem—identified with the effective horizon—and for the incoherent dispersive radiation generated through integrability-breaking dynamics, we demonstrated that the total entropy obeys a generalized second law, even though the underlying field evolution is governed by a Hamiltonian equation of motion. This establishes nonlinear fiber-based optical horizons as genuine nonequilibrium thermodynamic systems, rather than as purely kinematic or geometric analogs.

Conceptually, our results clarify that the emergence of a Hawking-like temperature in optical systems is inseparable from irreversible information transfer induced by mode coupling to dispersive continua. Entropy production is shown to originate from coarse-graining over dynamically generated radiation degrees of freedom, providing a concrete physical mechanism for irreversibility that does not rely on dissipation or coupling to an external bath. In this sense, soliton fission acts as an intrinsic entropy-generating process, closely paralleling semiclassical horizon physics where entropy growth arises from subsystem tracing rather than equilibration.

From an experimental perspective, the present framework opens a direct route to quantifying information entropy and irreversibility in laboratory analog gravity systems using measurable spectral observables. More broadly, it provides a platform for exploring the interplay between dispersion, dynamical backreaction, and thermodynamic laws in driven photonic systems. This extends analog gravity beyond horizon kinematics into the domain of quantum simulation, offering a controlled environment to probe the non-classical signatures of information scrambling and horizon recoil.

Acknowledgements

The author gratefully acknowledges the support of the Material Simulation Laboratory at Pamukkale University. The computational resources and research environment provided by the laboratory were instrumental in the completion of this work. The author also thanks U. R. Fischer, H. Zor Oguz and Z. M. Yuksel for valuable discussions and insightful comments.

References

- [1] W. G. Unruh. Experimental black-hole evaporation? *Physical Review Letters*, 46:1351–1353, 1981.
- [2] S. W. Hawking. Black hole explosions? *Nature*, 248:30–31, 1974.
- [3] L. J. Garay, J. R. Anglin, J. I. Cirac, and P. Zoller. Sonic analog of gravitational black holes in Bose-Einstein condensates. *Physical Review Letters*, 85:4643–4647, 2000.
- [4] J. Steinhauer. Observation of quantum Hawking radiation and its entanglement in an analogue black hole. *Nature Physics*, 12:959–965, 2016.
- [5] U. R. Fischer and Ralf Schützhold. Measurable quantum backreaction in ultracold gases. *Physical Review A*, 106:053319, 2022.
- [6] U. R. Fischer and Ralf Schützhold. Quantum simulation of cosmic inflation in two-component Bose-Einstein condensates. *Physical Review A*, 70:063615, 2004.
- [7] U. Leonhardt and P. Piwnicki. Relativistic effects of light in moving media with extremely low group velocity. *Physical Review Letters*, 84:822–825, 2000.
- [8] T. G. Philbin, C. Kuklewicz, S. Robertson, S. Hill, F. König, and U. Leonhardt. Fiber-optical analog of the event horizon. *Science*, 319(5868):1367–1370, 2008.

[9] F. Belgiorno, S. L. Cacciatori, M. Clerici, V. Gorini, G. Ortenzi, L. Rizzi, E. Rubino, V. G. Sala, and D. Faccio. Hawking radiation from ultrashort laser pulse filaments. *Physical Review Letters*, 105:203901, 2010.

[10] E. Rubino, F. Belgiorno, S. L. Cacciatori, M. Clerici, V. Gorini, G. Ortenzi, L. Rizzi, V. G. Sala, and D. Faccio. Negative-frequency resonant radiation. *Physical Review Letters*, 108:253901, 2012.

[11] W. G. Unruh. Sonic analogue of black holes and the effects of high frequencies on black hole evaporation. *Physical Review D*, 51:2827–2838, 1995.

[12] S. Robertson. The theory of Hawking radiation in laboratory analogues. *Journal of Physics B: Atomic, Molecular and Optical Physics*, 45:163001, 2012.

[13] J. D. Bekenstein. Black holes and entropy. *Physical Review D*, 7:2333–2346, 1973.

[14] J. D. Bekenstein. Generalized second law of thermodynamics in black-hole physics. *Physical Review D*, 9:3292–3300, 1974.

[15] U. R. Fischer and A. Tikar. Testing black hole scrambling with analogue Hawking radiation. *European Physical Journal C*, 82:10149–8, 2022.

[16] H. P. Breuer and F. Petruccione. *The Theory of Open Quantum Systems*. Oxford University Press, Oxford, 2002.

[17] N. Akhmediev and M. Karlsson. Cherenkov radiation emitted by solitons in optical fibers. *Physical Review A*, 51:2602–2607, 1995.

[18] D. V. Skryabin and A. V. Gorbach. Looking at the soliton through the prism of optical supercontinuum. *Reviews of Modern Physics*, 82:1287–1299, 2010.

[19] D. N. Page. Information in black hole radiation. *Physical Review Letters*, 71:3743–3746, 1993.

[20] G. P. Agrawal. *Nonlinear Fiber Optics*. Academic Press, Oxford, 5th edition, 2013.

[21] O. V. Sinkin, R. Holzlöhner, J. Zweck, and C. R. Menyuk. Optimization of the split-step Fourier method for simulating optical fiber communications systems. *Journal of Lightwave Technology*, 21(1):61–68, 2003.

[22] J. M. Dudley, G. Genty, and S. Coen. Supercontinuum generation in photonic crystal fiber. *Reviews of Modern Physics*, 78:1135–1184, 2006.

[23] C. Husko, M. Ruaud, G. Rey, I. Sagnes, S. Robertson, D. Faccio, S. Combrié, and A. De Rossi. Observation of solitonic optical event horizons. *Scientific Reports*, 3:1100, 2013.

[24] M. K. Parikh and F. Wilczek. Hawking radiation as tunneling. *Physical Review Letters*, 85:5042–5045, 2000.